Available online at www.sciencedirect.com

ScienceDirect

Procedia Manufacturing 17 (2018) 29–36

Procedia MANUFACTURING

www.elsevier.com/locate/procedia

28th International Conference on Flexible Automation and Intelligent Manufacturing (FAIM2018), June 11-14, 2018, Columbus, OH, USA

Topology optimization of 2.5D parts using the SIMP method with a variable thickness approach

Volkan Kandemir[a], Oguz Dogan[b,*], Ulas Yaman[c]

[a]*Department of Technological Devices and Process Department, ROKETSAN, Ankara 06780, Turkey*
[b]*Radar and Electronic Warfare Systems, ASELSAN, Ankara 06830, Turkey*
[c]*Department of Mechanical Engineering, Middle East Technical University, Ankara 06800, Turkey*

Abstract

In this study, the Solid Isotropic Material with Penalization (SIMP) topology optimization method is employed on the artifacts via keeping the penalization factor as unity. When the penalization is not carried out, the finite elements of the artifact have intermediate material densities. These density values are then used as the thicknesses of the corresponding finite elements and conformal surfaces are formed utilizing these heights in the proposed method. We evaluated the performance of the method with the conventional SIMP method, having penalization factors larger than one, in terms of numerical analysis and experiments. The results revealed that the proposed approach outperforms the classical SIMP method.

Keywords: Additive manufacturing; 3D printing; Topology Optimization; SIMP; FDM; FFF

1. Introduction

Due to the recent advancements in various technologies (CAD software, laser, servo systems, materials, etc.) Additive manufacturing (AM) is shifting from just producing prototypes to fabricating end products. According to the projections of Jiang et al. [1], we will be using AM machinery for reducing the carbon footprint of manufacturing and transformation of parts by 2030. Topology optimization in AM is one of the key technologies to

10.1016/j.promfg.2018.10.009

decrease the weight of the artifacts while satisfying the project requirements, which will result in less carbon generation. Although topology optimization has been studied for decades, such methods are becoming more visible with the advancements in AM industry. This is due to the difficulty in fabricating optimized parts via conventional manufacturing methods.

Various AM methodologies have been utilized to fabricate optimized artifacts. The most commonly used methods are Powder Bed Fusion (PBF) based processes due to their ability to fabricate metal-based materials. Another reason is the self-supporting ability of PBF processes. Fused Filament Fabrication (FFF) [2] has also been studied frequently for topology optimization purposes in the recent years due to their low cost and various configurations. These studies mostly focus on the optimization of interior structures [3] and support structures [4]. With the introduction of high strength (ABS Plus, PC, Onyx, etc.) and special support structure materials (PVA, Breakaway, etc.) for FFF process, we will be using FFF for the fabrication of topologically optimized critical parts more in the near future. In this study, we also fabricated our parts utilizing FFF based 3D printers.

There are different topology optimization methods that can be employed for AM in the literature [5]. Solid Isotropic Material with Penalization (SIMP) [6] method is one of the popular ones and it simply distributes the available material to the grids depending on the results of the Finite Element Analysis (FEA). The second one is a truss-based method, namely Ground Structure Method [7]. It reduces the number of trusses from a high-density truss network. The last group of methods utilize genetic algorithms to obtain the optimum truss structures [8] or optimum distribution of solid grids [9]. With the help of these methods, various mechanical properties (strength, deflection, etc.) of the objects can be improved with respect to the conventional way of design and manufacturing. We used the SIMP method in this study with different penalization parameters to increase the strength to weight ratio of the parts.

The SIMP algorithm for topology optimization avoids the formation of regions having intermediated densities. Formation of void and solid regions are encouraged by penalizing the intermediate densities. As discussed in [10], this penalization means that the optimized topology is less optimal than the case where the intermediate densities had not been penalized. If there were a way to manufacture these intermediate regions, there would be no need to penalize them. For that purpose, the intermediate densities can be mapped to lattice structures of varying volume fractions. Although, these approaches bring a good solution for intermediate density regions, such structures are hard to fabricate. The printer resolution is the limiting factor for fabrication of these microstructures. Relative Density Mapping, which is a similar approach, was suggested by [11] which uses relative density information from the optimization. In this method, density information is mapped onto the predefined lattice configurations. Another way of dealing with the intermediate densities is to utilize multiple materials. These intermediate densities can be considered as different materials having different densities. However, material that can be available would be quite limited to provide varying densities.

In this study, we proposed a new approach for intermediate densities as Variable Thickness Approach. The thickness of each point of the optimized part is proportional to the density ratio at that point. The main objective of the study is to represent topologically optimized 2.5D parts with formed surfaces and generate 3D printable models in an automatic manner. The use of variable thickness (formed surfaces) throughout the part increases the manufacturability and the mechanical properties of them due to the continuity of the layers. There are no truss-like structures in the optimized shapes as opposed to the most of the methods discussed in the literature.

The rest of the paper is organized as follows. The next section discusses the proposed method on the fabrication of topologically optimized artifacts. Then in the third section, numerical analysis of the test cases is performed and compared with each other. After discussing the results of three-point bending tests performed in the fourth section, the paper is concluded with the last section.

2. Proposed method

In order to justify the validity of the proposed method, a comparison between two similar bodies is done with FEA. The only difference between these two bodies is that there is a thin mid layer on the second part as illustrated in Fig. 1. Each body is fixed on the ground at the left end and the same unit load is applied on the right end. As seen from Fig. 2, the deflection on the first body is about 1.5 times higher than the deflection on the second part, but the second body is just 5% heavier than the first one. The body on the left behaves like two different beams fixed at the end. Whereas, the second one behaves like an *I* beam. Moreover, when the Section A-A and Section B-B are

compared in terms of their second moment of the areas on z-axis, i.e. I_{zz}, it is clear that the second body has a larger second moment of area because of the shape of the *I* beam. Therefore, it will deflect less under the same load and resist to higher loads. On the contrary, the results of the SIMP method are mostly converted to truss like structures, similar to the second shape, and it contains discontinuities. Hence, their load carrying capacities are decreased significantly. We proposed a new method in order to obtain an optimized structure similar to the first shape. In this method, the continuity of the shape is conserved by keeping the penalization factor at unity and setting zero threshold value for the density. The density difference is reflected on the artifact by changing the thickness of the part at each point.

2.1. Model Generation

CAD model of the optimized geometry is obtained in several steps as summarized in Fig. 3. As a first step, TopOpt add on [12] is used in Grasshopper3D to analyze and obtain the density distribution in the defined domain with the applied boundary conditions. This density ratio can be evaluated in different ways to obtain an optimized structure. Basically, filtering can be used as a threshold to decide on the portion of the domain to be eliminated. Truss like structures are mostly obtained by using this method. Alternatively, a mapping in between the density ratios and the microstructures can be used, but the manufacturability of these microstructures can be challenging. As a third alternative, different thicknesses are assigned to each point in the domain proportional to their density values. These thickness values correspond to the z-values of the points, which will be used to generate a surface. Then, the surface is used to trim the part which was obtained by extruding the initial domain in Rhinoceros3D environment. For all the methods, parts are exported as STL files to be fabricated on FFF type of 3D printers.

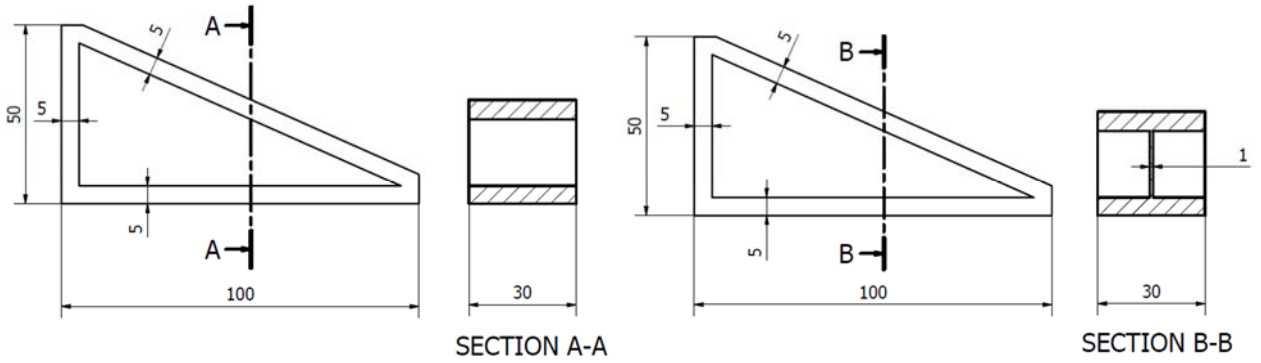

Fig. 1. (a) Truss structure; (b) Truss structure with a mid-layer.

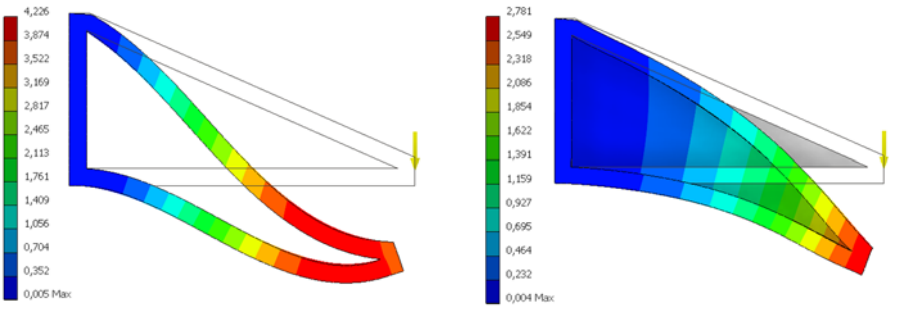

Fig. 2. (a) FEA result of truss structure; (b) FEA result of truss structure with a mid-layer.

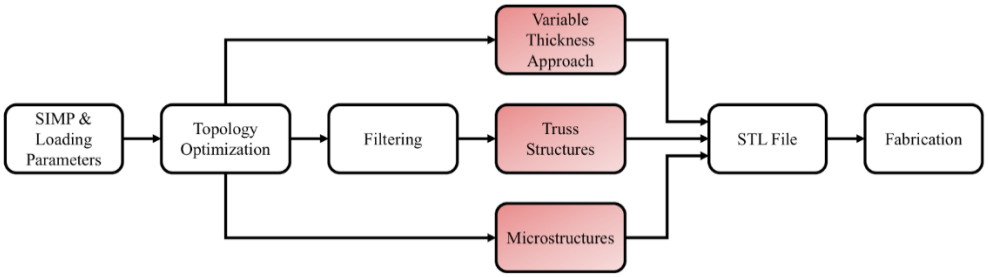

Fig. 3. Design and fabrication pipeline of the proposed methods.

2.2. Test Parts

Eight different parts are manufactured, analyzed and tested in this study as designated in Table 1. The printed parts with ABS and ONYX are provided in Fig. 4. Five of them are based on the traditional method and other three (P1SH, P1SV, P3S) are generated via the proposed approach. Target value for the volume fraction is 50% and the threshold value for the truss like structures are calculated based on this goal. First of all, a fully filled beam is fabricated as a reference. Secondly, triangularly half-filled part is fabricated, which is the default method suggested by the printer companies to save material and time. Then other parts are obtained based on topology optimization. To take the benefit of the proposed method, penalization factor should be taken as unity. In other words, no penalization should be applied during the optimization to reveal the advantages of the presented approach. Therefore, for the unity penalization factor, three parts are manufactured. The first one is obtained by using the traditional SIMP method. Whereas, other two are generated with the proposed method employing different printing orientations to see the effect of the orientation on the strength of the parts. On the other hand, penalization factor is usually taken as three (default value of the SIMP implementations) to obtain good-looking truss like shapes. Therefore, we also take the penalization factor as three to fabricate two trusses. One of them is according to the SIMP method and the other one is printed via variable thickness approach. Finally, the same part is modelled with microstructures. To do that, after the topology optimization, every cell on the domain is converted to a microstructure according to the densities they have. Four type of microstructures, as given in the Table 2, are used for this study and all of them have a square shape since they can be manufactured easily on FFF type of 3D printers. The first type of the microstructures is completely filled and it is used on the cells whose densities are more than 75%. The second and the third types of the microstructures are hollow squares and the wall thicknesses of these microstructures are designed according to the nozzle diameter of the printers. Lastly, the places whose densities are less than 25% are left as blank. To sum up, we fabricated these eight different parts utilizing two different materials (ABS from Ultimaker and ONYX from Markforged) on two different 3D printers. Fabrication parameters used in this study are provided in Table 3.

Table 1. Test coupon designations.

Materials	Structure Type	
ABS	CF	Completely filled, 100% material
ONXY	HF	Half filled, 50% material
	M	Microstructure
	P3T	Penalization=3, Truss type
	P3S	Penalization=3, Variable Thickness Approach
	P1T	Penalization=1, Truss type
	P1SH	Penalization=1, Variable Thickness Approach, Horizontally manufactured
	P1SV	Penalization=1, Variable Thickness Approach, Vertically manufactured

Table 2. Properties of the microstructures

Properties	First (Fully filled)	Second (Hollow square)	Third (Hollow square)	Fourth (Blank)
Outer edge length (mm)	5	5	5	NA
Inner edge length (mm)	NA	2	3.4	NA
Wall thickness (mm)	NA	1.5	0.8	NA
Area (mm^2)	25	21	13.44	0
Area ratio (%)	100	84	54	0
Used places for densities	0.75-1	0.5-0.75	0.25-0.5	0-0.25

Fig. 4. Test coupons (a) ABS-CF, (b) ABS-HF, (c) ABS-P1T, (d) ABS-P1SH, (e) ABS-P1SV, (f) ABS-P3T, (g) ABS-P3S, (h) ABS-M, (i) ONXY-CF, (j) ONXY-HF, (k) ONXY-P1T, (l) ONXY-P1TSH, (m) ONXY-P1SV, (n) ONXY-P3T, (o) ONXY-P3S, (p) ONXY-M

Table 3. Fabrication parameters

Properties	Markforged Mark Two	Ultimaker 3 Extended
Layer thickness (mm)	0.1	0.1
Nozzle diameter (mm)	0.4	0.4
Shells	3	3
Build table temperature (°C)	NA	80

3. Analysis

The 3D models of the samples are imported into ABAQUS for finite element simulation of elastic deformation under 3-point bending test. The simulation is performed with implicit scheme. The material is assumed to be homogeneous and isotropic in nature. The material properties are obtained from the websites of the manufacturers. Analysis are limited to the elastic regime since no data available for the plastic regime. Therefore, the applied force is selected such that the maximum stress created within the body is much smaller than the tensile limits of the materials. C3D10 (10-node quadratic tetrahedron) element is used to mesh the specimens since we have complex surfaces. The meshing of the model with tetrahedron elements is shown in Fig. 5. The applied load and the simply supported boundary conditions are also shown in the same figure. The beam is pinned to its supports at both ends; it cannot experience deflection at these ends. However, the beam is free to rotate around z-axis and does not experience any torque.

Analyses are performed for CF, P1T, P1S, P3T and P3S models. On the other hand, analysis is not practically applicable for the remaining models due to their intricate shapes. The applied load vs maximum deformation data are given in Table 4. The applied load is intentionally selected as specified in order to have 3 mm of deflection for each model. None of the parts exceeds their tensile limits at those specified loads.

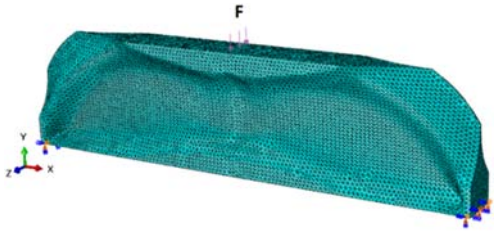

Fig. 5. Meshed test specimen.

Table 4. Applied forces in order to have 3 mm deflection in each specimen.

Model	Applied Force [N]	
	ABS	ONXY
CF	2276	1896
P1T	341	284
P1S	1587	1323
P3T	1440	1200
P3S	1433	1194

Table 5. Weight of the specimens and Applied Load / Weight indices for ABS / ONYX

Model	Weight [N] (calculated)	Load / Weight [N/N]
CF	0.37 / 0.42	6195 / 4550
P1T	0.18 / 0.20	1910 / 1401
P1S	0.18 / 0.20	8913 / 6549
P3T	0.18 / 0.21	7877 / 5784
P3S	0.17 / 0.20	8190 / 6017

For ABS and ONXY, completely filled models withstand to higher loads for 3 mm deformation specifications as expected. However, the loads they carry for 3 mm deformation can be scaled to their weights to have more meaningful results for the weight saving point of view. Load/weight indices can be interpreted as specific load carrying capacities of the specimens in the elastic regime, which is a better way of comparing the performance of each model. In that case, P1S models for both ABS and ONXY come into prominence when load/weight index are taken into account as summarized in Table 5. These results show that the performance of Variable Thickness Approach in Topology Optimization with SIMP is outstanding.

4. Tests

The three-point bending tests are conducted in order to compare the strength of the alternative solutions. In this three-point bending test, the test specimen is placed in a support structure, which is attached to Lloyd LR100K Plus machine as shown in Fig. 6. Then, the simply supported test specimen is loaded until it is broken. At the start of the test, the specimen is at an undeformed state. However, the crosshead makes contact with the specimen with a small preload (< 1 N) in order to keep the specimen in place. The crosshead moves downward at a rate of 4 mm/min. The applied load is increased as crosshead moves downward. Load (F) and displacement (d) values are recorded simultaneously during the tests and the load carrying capacities of each specimen is determined.

Test results are evaluated in the elastic regime since the properties of the materials in the plastic regime are not available. Moreover, the technical datasheet of ONXY states that flexural strain at break is not available because neither material breaks before the test ends [13]. We exactly encountered the same problem with ONXY test specimens. Therefore, we limit our investigation with the elastic zone. The applied load at 3 mm deflection are tabulated in Table 6. The completely filled models carry higher loads as expected. The load carrying capacity of P1S is the best among the all optimized parts in accordance with analysis results. Moreover, P1S models show better performance when load/weight index is considered.

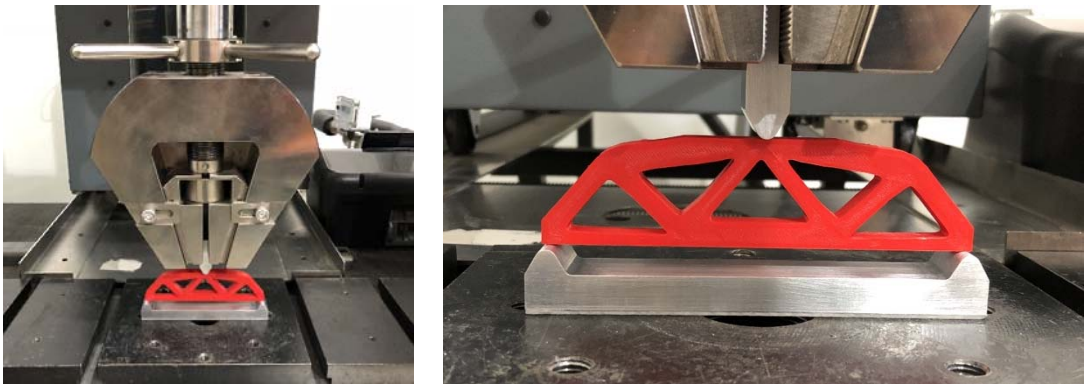

Fig. 6. Test setup Lloyd LR100K Plus machine

There is a discrepancy between the test forces and the analysis forces at specific deformation level. It is considered that these differences arise from the manufacturing process. Material is assumed to be homogeneous and isotropic in the analysis. However, FFF parts exhibit orthotropic properties like composites [14]. The difference between the load capacity of P1SH and P1SV is a good evidence of the effect of manufacturing process. However, it is impossible to observe the difference of load carrying capacities of P1SH and P1SV test pieces through the FEA.

Table 6. Comparison of forces at 3mm of deflection for ABS / ONYX

Model	Mass [gr]	Test Force [N]	Analysis Force [N]	Error %	Load / Weight Index
CF	37.5 / 39.8	2245 / 2278	2280 / 1896	1.5 / 16.8	6103 / 5834
HF	26.6 / 20.4	1475 / 637	- / -	- / -	5653 / 3183
P1T	19.5 / 20.0	364 / 317	340 / 283	6.6 / 10.7	1903 / 1616
P1SV	20.2 / 20.4	1911 / 1454	1590 / 1323	16.8 / 9.0	9644 / 7265
P1SH	19.7 / 20.2	1783 / 1790	1590 / 1323	10.8 / 26.1	9226 / 9033
P3T	19.6 / 20.7	1685 / 1683	1448 / 1200	14.0 / 29.1	8763 / 8337
P3S	20.2 / 20.2	1810 / 1281	1440 / 1194	20.4 / 6.8	9134 / 6464
M	26.1 / 26.1	1423 / 717	- / -	- / -	5558 / 2800

5. Conclusions

In this study, we proposed a novel approach on 3D printing of topologically optimized artifacts with the SIMP method. We did take the penalization parameter in the SIMP as unity and made use of the densities of each grid to prepare ready-to-print 3D models. Although our method starts with 2.5D objects, the resulting artifacts have conformal surfaces when variable thickness approach is followed. Considering the results of the tests performed, our method improves the load/weight index by around five times (P1S vs P1T). As future works, we plan to focus more on the microstructures, multi-material applications, and direct slicing. In direct slicing, we will be generating G-codes within the Grasshopper3D environment. In that case, there will be no need to generate STL files whose sizes would increase tremendously when microstructures are embedded into the model.

References

[1] R. Jiang, R. Kleer, F.T. Piller, Predicting the future of additive manufacturing: A Delphi study on economic and societal implications of 3D printing for 2030, Technological Forecasting and Social Change 117 (2017) 84-97.
[2] R. Rezaie, Topology optimization for fused deposition modeling process, Procedia CIRP 6 (2013) 521-526.
[3] N. Gardan, A. Schneider, Topological optimization of internal patterns and support in additive manufacturing, Journal of Manufacturing Systems 37 (2015) 417-425.
[4] M. Langelaar, Topology optimization of 3D self-supporting structures for additive manufacturing, Additive Manufacturing 12 (2016) 60-70.
[5] Z. Tomás, G.H. Paulino, Bridging topology optimization and additive manufacturing, Structural and Multidisciplinary Optimization 53.1 (2016) 175-192.
[6] M.P. Bendsøe, O. Sigmund, Material interpolation schemes in topology optimization, Archive of applied mechanics 69.9-10 (1999) 635-654.
[7] M.P. Bendsøe, A. Ben-Tal, J. Zowe, Optimization methods for truss geometry and topology design, Structural optimization 7.3 (1994) 141-159.
[8] H. Kawamura, H. Ohmori, N. Kito. Truss topology optimization by a modified genetic algorithm, Structural and Multidisciplinary Optimization 23.6 (2002) 467-473.
[9] S.Y. Wang, K. Tai, Structural topology design optimization using genetic algorithms with a bit-array representation, Computer methods in applied mechanics and engineering 194.36-38 (2005) 3749-3770.
[10] D. Brackett, I. Ashcroft, R. Hague,Topology optimization for additive manufacturing. In Proceedings of the solid freeform fabrication symposium, 1 (2011) 348-362.
[11] M. Alzahrani, Design of truss-like cellular structures using density information from topology optimization, Doctoral dissertation, Georgia Institute of Technology, (2014).
[12] TopOpt Plugin for Grasshopper3D, http://www.topopt.dtu.dk/?q=node/908, last accessed: February 11, 2018.
[13] Material properties of ONYX, https://support.markforged.com/hc/en-us/articles/209934486-Onyx, last accessed: February 11, 2018.
[14] A. Gianluca, M. Stefania M, C. Luca, A. Ferdinando, Influence of meso-structure and chemical composition on FDM 3D-printed parts, Composites Part B 113 (2017) 371 – 380.